Implementation of intensity-modulated laser diodes in time-resolved, pump–probe fluorescence microscopy

Chen-Yuan Dong, Christof Buehler, Peter T. C. So, Todd French, and Enrico Gratton

We present the implementation of intensity-modulated laser diodes for applications in frequency-domain pump–probe fluorescence microscopy. Our technique, which is based on the stimulated-emission approach, uses two sinusoidally modulated laser diodes. One laser (635 nm) excites the chromophores under study, and the other laser (680 nm) is responsible for inducing stimulated emission from excited-state molecules. Both light sources are modulated in the 80-MHz range but with an offset of 5 kHz between them. The result of the interaction of the pump and the probe beams is that a cross-correlation fluorescence signal at 5 kHz is generated primarily at the focal volume. Microscope imaging at the cross-correlation signal results in images with high contrast, and time-resolved high-frequency information can be acquired without high-speed detection. A detailed experimental arrangement of our methodology is presented along with images acquired from a 4.0-μm-diameter fluorescent sphere and TOTO-3–labeled mouse STO cells. (TOTO-3 is a nucleic acid stain.) Our results demonstrate the feasibility of using sinusoidally modulated laser diodes for pump–probe imaging, creating the exciting possibility of high-contrast time-resolved imaging with low-cost laser-diode systems.

OCIS codes: 180.0180, 140.2020, 170.2520.

1. Introduction

In spectroscopy the development of pump–probe techniques has led to the understanding of many ultrafast phenomena. Subpicosecond processes in biology, condensed matter, and chemistry have been probed by use of the pump–probe technology. In a typical implementation, laser beams with a short pulse width are split and recombined at the sample of interest. By the use of an optical delay line, the temporal separation between the two beams can be controlled and time-dependent processes of the sample studied. Monitoring the probe-beam intensity profile at different pulse separations allows ultrafast phenomena to be studied without ultrafast photodetectors. The concept of converting the spatial separation in a pulse delay into temporal studies of ultrafast phenomena is central to the pump–probe technique, and ultrafast phenomena can be studied in this manner.[1–3] In this methodology the temporal resolution is often determined by the temporal profile of the laser source. Recent developments in technology have led to lasers with pulse durations in the less than 10-fs range.[4–6] In biology pump–probe methodology has been valuable in studying systems such as heme proteins, photosynthetic reaction centers, and rhodopsin.[7]

In addition to the optical delay-line approach, there exists an alternative technique proposed by Elzinga and co-workers.[8,9] In this asynchronous-sampling technique two pulsed lasers at high repetition frequencies are focused to a common spot on the sample. One laser (the pump) excites the sample, whereas the second laser (the probe) can be used to probe the population of the ground state or to induce stimulated emission from excited-state molecules. The key to this methodology is that the repetition fre-

When this research was performed, C.-Y. Dong (chen@lfd.physics.uiuc.edu) and P. T. C. So were with the Department of Mechanical Engineering, Massachusetts Institute of Technology, 77 Massachusetts Avenue, Cambridge, Massachusetts 02139. C.-Y. Dong is now with the Department of Physics, National Taiwan University, Taipei, Taiwan 106. C. Buehler is with the Paul Scherrer Institut (PSI), WHMA/C24 Ch-5232 Villigen PSI, Switzerland. T. French is with LJL Biosystems, 404 Tasman Drive, Sunnyvale, California 94089. E. Gratton is with the Department of Physics, University of Illinois at Urbana-Champaign, 1110 West Green Street, Urbana, Illinois 61801.

Received 1 June 2000; revised manuscript received 29 September 2000.

0003-6935/01/071109-07$15.00/0

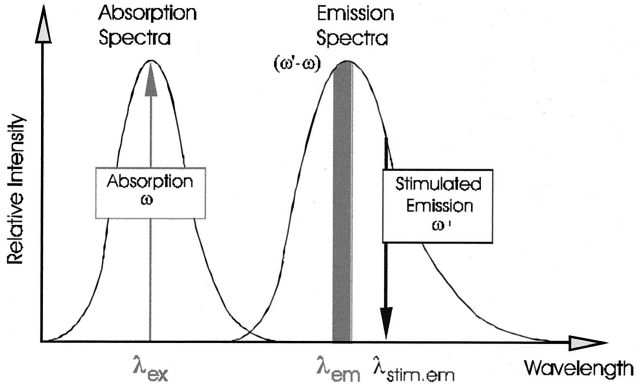

Fig. 1. Frequency-domain pump–probe technique based on the principles of stimulated emission. stim.em, stimulated emission.

quencies of the two lasers are offset from each other by a small amount. The result is that a continually varying delay is generated between the pump and the probe pulses. In the frequency domain the continual probing of the sample dynamics at multiple times after the arrival of the pump beam leads to the generation of a cross-correlation signal that contains the signal (at the fundamental cross-correlation frequency) and its harmonics. The cross-correlation signal can then be analyzed to obtain time-resolved information about the sample.

Unlike the transient approach in which both the pump and the probe lasers are used to excite the sample, the wavelength of the probe beam in the stimulated-emission approach is used to induce stimulated emission from the excited-state molecules. Monitoring the fluorescence change induced by the probe beam means that ground-state depletion, as in transient absorption, is not necessary and that photobleaching is greatly reduced. The stimulated-emission approach has been demonstrated in both microscopic and spectroscopic studies.[10–14]

2. Generation of the Low-Frequency Cross-Correlation Signal and Its Consequences

A. Derivation of the Low-Frequency Cross-Correlation Signal

The basic principles of the pump–probe (stimulated-emission) approach are illustrated in Fig. 1. Shown in the figure are the absorption and the emission spectra of a hypothetical fluorescent species. Because typical flurorophores in solution have at least an approximately 50-nm separation between the absorption and the emission maxima, the wavelengths of the pump and the probe lasers can be selected for excitation and inducing stimulated emission, respectively, without the two processes interfering with each other. The pump beam can be modulated at an angular frequency of ω, and the probe beam can be modulated at a slightly different angular frequency of ω'. The result of continually exciting and de-exciting the fluorescent molecules is that the two frequencies are mixed in the excited-state population, and, as a result, both the sum $\omega' + \omega$ and the difference $\omega' - \omega$ frequency signals are generated in the fluorescence. Detection at the $\omega' - \omega$ low-frequency signal can provide time-resolved information at the high-frequency excitation signal ω.

To understand the generation of the cross-correlation signal and the advantages of using it for microscopic imaging, consider the spatial $\mathbf{r}$ and the temporal t behaviors of the excited-state population density $N(\mathbf{r}, t)$ under the pump–probe action, as given by

$$\frac{dN(\mathbf{r}, t)}{dt} = -\frac{1}{\tau}N(\mathbf{r}, t) + \sigma(\lambda)I(\mathbf{r}, t)[c - N(\mathbf{r}, t)] - \sigma'(\lambda')I'(\mathbf{r}, t)N(\mathbf{r}, t), \quad (1)$$

where τ is the excited-state lifetime, c is the molecular concentration, and $\sigma(\lambda)$ and $\sigma'(\lambda')$ are the wavelength-dependent absorption and the stimulated-emission cross sections, respectively. In the case in which the pump and the probe beams have sinusoidal temporal dependence their intensity profiles are respectively represented as $I(\mathbf{r}, t) = I(\mathbf{r})\cos(\omega t)$ and $I'(\mathbf{r}, t) = I'(\mathbf{r})\cos(\omega' t)$. In Eq. (1) the dynamics of the excited population are dictated by three phenomena: First, the excited-state molecule can undergo decay, as represented by $-(1/\tau)N(\mathbf{r}, t)$. Second, the ground-state molecules can absorb the exciting photons and reach the excited state, as in $\sigma(\lambda)I(\mathbf{r}, t)[c - N(\mathbf{r}, t)]$. Finally, the term $-\sigma'(\lambda')I'(\mathbf{r}, t)N(\mathbf{r}, t)$ is responsible for excited-state depletion through the process of stimulated emission. In the absence of the probe beam Eq. (1) then describes the standard excited-state response under the excitation of $I(\mathbf{r}, t)$.

The sinusoidal solution for Eq. (1) was addressed[14] previously. Because the fluorescence distribution is related to the excited-state population and the quantum yield q by $F(\mathbf{r}, t) = -q\,dN(\mathbf{r}, t)/dt$, the solution to Eq. (1) can be used to obtain the low-frequency cross-correlation fluorescence signal:

$$F_{cc}(t) = \frac{qc\tau\sigma(\lambda)\sigma'(\lambda')}{2}\frac{1}{(1 + \omega^2)^{1/2}}\cos[(\omega' - \omega)t - \phi] \times \int I(\mathbf{r})I'(\mathbf{r})d^3\mathbf{r}. \quad (2)$$

Equation (2) clearly shows that the time-resolved response of the molecular system can be obtained from the amplitude term, which contains $1/(1 + \omega^2\tau^2)^{1/2}$, or the phase ϕ, which is related to the lifetime and the angular frequency by $\tan(\phi) = \omega\tau$. As was discussed above, there is also a high-frequency cross-correlation signal at the sum frequency $\omega' + \omega$. But because the sum frequency is at an even higher frequency than is the excitation frequency ω, it is only logical that the difference-frequency signal $\omega' - \omega$ be analyzed for time-resolved information.

B. Consequences of the Spatial and the Temporal Dependence of the Cross-Correlation Signal

Two important results can be concluded from Eq. (2): First, fluorescence imaging at the cross-correlation frequency results in localized observation of the focal volume, leading to images with enhanced axial depth discrimination and therefore superior image contrast. Second, high-frequency time-resolved imaging without using high-speed photodetectors is feasible.

Equation (2) shows that the cross-correlation signal depends on the spatial integral of the product of the pump and the probe beams' spatial profile:

$$\int I(\mathbf{r})I'(\mathbf{r})\mathrm{d}^3\mathbf{r}.$$

In other words, the point-spread function (PSF) of the pump–probe imaging scheme is $I(\mathbf{r})I'(\mathbf{r})$. Expressed in the dimensionless axial and radial coordinates of $u = 2\pi(\mathrm{NA})^2 z/\lambda$ and $v = 2\pi(\mathrm{NA})r/\lambda$, the PSF becomes

$$I(u, v)I'(u', v'), \tag{3}$$

where

$$I(u, v) = \left| 2\int_0^1 J_0(v\rho)\exp(-iu\rho^2/2)\rho\mathrm{d}\rho \right|^2,$$

as derived in Refs. 15–17. Note that the pump–probe PSF, as indicated by expression (3), is remarkably similar in form to the PSF in two-photon microscopy, as given by $I^2(u/2, v/2)$ and is identical to the PSF in confocal microscopy if the probe-beam wavelength is the same as the confocal detection wavelength.[18] Therefore one would expect the same axial depth discrimination as in two-photon and confocal microscopy to be a characteristic for pump–probe microscopy also. However, compared with the other two techniques, the nature of the axial depth discrimination in pump–probe microscopy has a different origin. In pump–probe microscopy, the cross-correlation signal is generated at the focal volume at which both the pump and the probe lasers have high intensities. The linear dependence of the pump–probe signal on either the pump or the probe power is expected because, to the lowest order, the number of excited-state molecules responsible for the cross-correlation signal is proportional to both the excitation strength and the effectiveness of de-excitation. Therefore, axial depth discrimination is achieved in pump–probe fluorescence microscopy, and image contrast is improved compared with conventional fluorescence techniques.[13]

Implied in Eq. (2) is the second important feature of the pump–probe methodology. Because the high-frequency lifetime information is translated to the low-frequency cross-correlation signal at $\omega' - \omega$, fast photodetectors are not necessary for high-frequency studies. In our study ω and ω' are both in the 80-MHz range. However, their difference, $\omega' - \omega$, can be chosen to be in the kilohertz range. Even for very-high-frequency time-resolved studies the difference frequency can still be chosen to be in the kilohertz range. As a result, standard photodetectors such as photomultiplier tubes (PMT's) can be used for high-frequency studies.

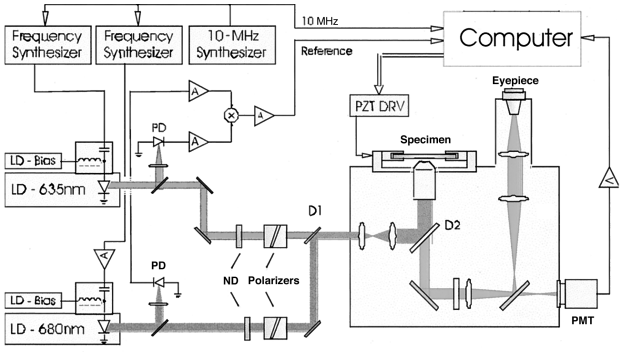

Fig. 2. Design of a pump–probe fluorescence microscope that uses intensity-modulated laser diodes. D1 and D2, dichroic mirrors; LD, laser diode; PD, photodetector; ND, neutral-density filter; PZT DRV, piezoelectric driver; A, amplifier.

C. Motivation for Using Laser Diodes in Pump–Probe Methodology

In previous implementations of pump–probe stimulated-emission microscopy the frequency content of pulsed laser systems was explored to extract time-resolved information from fluorescent systems.[12,14] Although pulsed systems are effective multiharmonic pump and probe sources, they are often available only as large and expensive units that require regular maintenance. Our motivation in introducing intensity-modulated laser diodes as pump and probe sources is to economize and improve the pump–probe technology. In the red–near-IR spectral range laser diodes are readily available as stable and low-cost units. They are also stable, reliable, and compact units that can be integrated easily into a pump–probe apparatus. With the eventual availability of blue–green laser diodes as promising low-cost laser sources, pump–probe imaging can become a popular alternative to existing technologies as a unique technique for providing time-resolved fluorescence images with excellent axial depth discrimination.

3. Experimental Apparatus

The experimental implementation of a laser-diode-based pump–probe microscope is shown in Fig. 2. A 10-MHz master synthesizer provides the synchronization signal for the system. Laser-diode modulation (by two independent synthesizers), piezoelectric-driven raster scanning of the sample, and PMT signal digitization are all synchronized to the same 10-MHz clock. We used two custom laser diodes (Power Technology, Inc., Mabelvale, Arkansas) emitting at different wavelengths as the pump and the probe sources. One laser diode, lasing at 635 nm [Model APM08(635-08)], is used for excita-

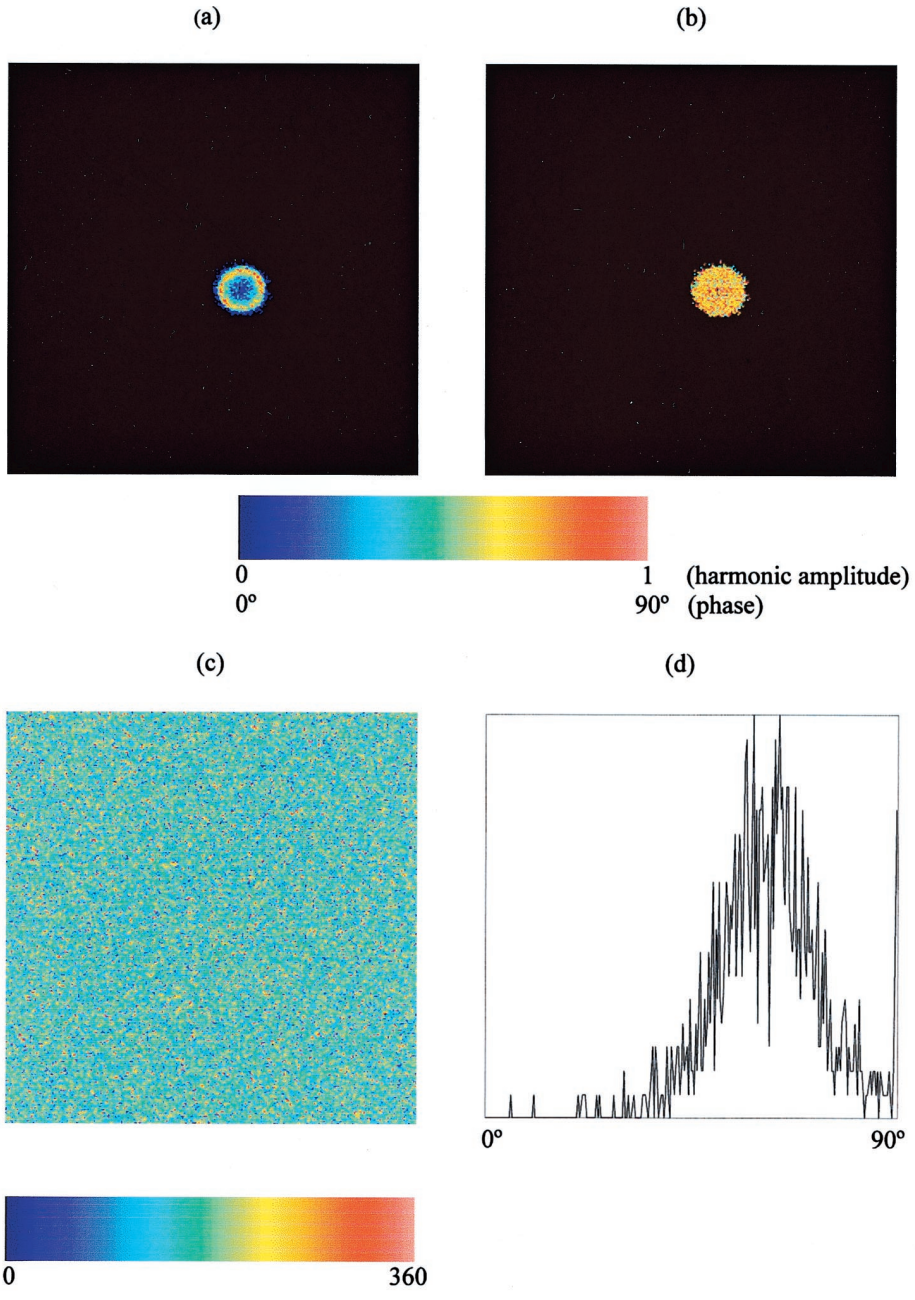

Fig. 3. Pump–probe time-resolved image of a Crimson FluoSphere (4.0-μm diameter): (a) The harmonic amplitude of the cross-correlated signal. (b) The lifetime phase of the sphere at 80 MHz (τ = 3.59 ns). (c) Phase image of the reference compound Nile Blue. (d) Phase histogram of the sphere; the y axis represents the relative contribution of the plotted phase value.

tion. The other unit [Model APM08(690-40)], operating at 680 nm, induces stimulated emission from the excited-state molecules. The dc biases of the laser diodes are provided by two independent, home-built current sources. The dc signal is combined with the modulation through a gigahertz Bias-T (Mini-Circuits, Brooklyn, New York, Model PBTC-1G). The output of the laser diodes can be modulated from approximately 10 to 150 MHz. The high-frequency limit is imposed primarily by the long connections between the laser diodes and the module case. In our experiments, we chose 80 MHz and 80 MHz + 5 kHz to be the pump and the probe frequencies, respectively.

A reference signal is derived from the output of the two laser diodes. Outputs of the laser diodes are detected by two independent photodiodes and are heterodyned by a balanced mixer (Mini Circuits, Model ZAD 3SH). The frequency-mixed signal is further amplified and is then used as the reference signal of our detection system. Such a referencing scheme allows us to compensate for any relative phase drifts between the two independently modulated laser systems.

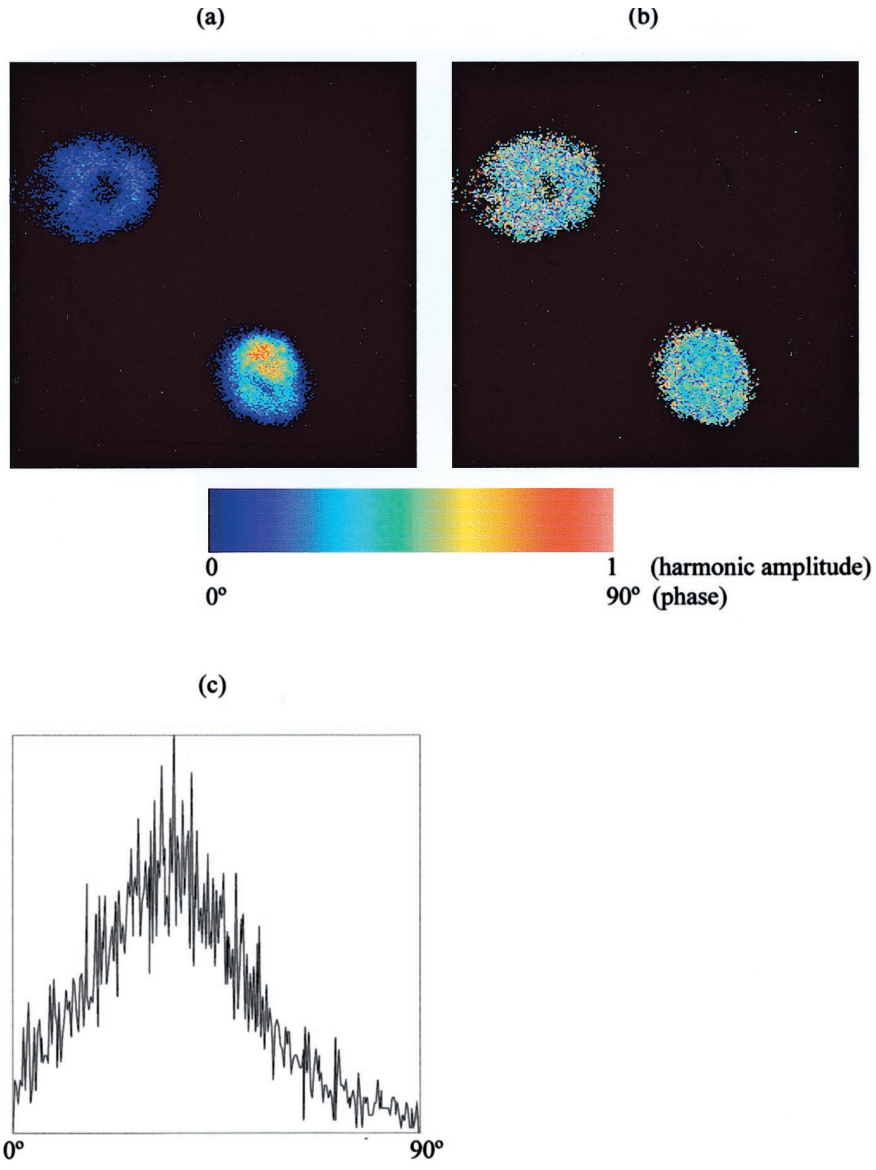

Fig. 4. Pump–probe time-resolved image of mouse STO cells that are labeled with the nucleic acid stain TOTO-3: (a) The harmonic amplitude of the cross-correlated signal. (b) The lifetime phase of the labeled nuclei at 80 MHz [τ = 1.81 ns (estimated)]. (c) Phase histogram of the labeled cells; the y axis represents the relative contribution of the plotted phase value.

Optically, the pump and the probe laser diodes are combined by a first dichroic mirror (Chroma Technology, Brattleboro, Vermont), see Fig. 2, and directed into our home-built microscope. This dichroic mirror combines the two beams by the transmission and the reflection of the 635- and the 680-nm lasers, respectively. The advantage of such a home-built design is that a minimum number of optical elements is used, thus maximizing the optical throughput of our system. The combined laser beams are further expanded before being reflected into the microscope objective by a second dichroic mirror (Chroma Technology, Brattleboro, Vermont), as shown in Fig. 2. Such beam expansion ensures the overfilling of the objective's back aperture, resulting in the generation of a diffraction-limited spot at the focal volume. The objective that we used is a high-numerical-aperture (1.25), 63× oil-immersion objective (Carl Zeiss, Inc., Thornwood, New York, Model Plan-Neofluar). At the sample the pump and the probe laser powers are approximately 0.5 and 3–4 mW, respectively. In our epi-illuminated setup the same objective that is used for focusing also collects the fluorescence signal, which contains the cross-correlation signal. A piezoelectric-driven sample stage is used for sample mounting and scanning. The acquired images are composed of 256 × 256 pixels and extend 50 μm along each radial axis.

The collected fluorescence passes through mirror D2 and optical filters before reaching the PMT. The output of the PMT is amplified, electronically filtered (5 ± 1 kHz), and further amplified to isolate the cross-correlation signal. The cross-correlation signal is then directed into a dual-channel, 12-bit, 100-

kHz digitizer (DRA Laboratories, Sterling, Virginia, Model A2D-160). Typical signal digitization involves the processing of 4 points/waveform. Although a minimum of only two digitization points is required to determine a sinusoidal signal, our digitization scheme samples 4 data points/waveform to further reduce harmonic noise and enhance the cross-correlation signal. At 5-waveform integration at each pixel the scanning time is 1 ms/pixel, corresponding to a frame-acquisition time of 65.5 s. Images acquired in this manner are collected and displayed by the data-acquisition computer. For reducing phase noise the signal generated by the direct monitoring of the laser-diode outputs is also processed by the computer and is used as the reference source.

4. Results and Discussion

In our experiments, we chose to demonstrate the feasibility of laser-diode-based pump–probe microscopy by imaging two systems: fluorescent microspheres and nuclei-labeled mouse STO cells. The fluorescent-sphere system that we chose was the 4.0-μm Crimson FluoSpheres system (Molecular Probes, Inc., Eugene, Oregon). The spectral properties of these spheres (an excitation maximum of 625 nm and an emission maximum of 645 nm) matches well with the excitation and the de-excitation wavelengths, respectively, of our laser diodes. To satisfy the magic-angle[19] condition, we scanned these spheres with the probe beam oriented at 54.7° relative to the pump laser.

The pump–probe scan of one such fluorescent sphere is shown in Fig. 3. To determine the lifetime from the phase image, we used the fluorescent species Nile Blue as a reference compound. The sphere's harmonic amplitude and phase images, along with the Nile Blue phase, are all shown in Fig. 3. From the phase image and the relation $\tan(\phi) = \omega\tau$, the lifetime of the sphere is determined to be 3.59 ns. The lifetime of Nile Blue in ethanol was determined to be 1.54 ns ($\phi = 37.7°$) by use of a conventional lifetime fluorometer (ISS, Champaign, Illinois, Model Koala). In this arrangement a pulsed laser system based on a frequency-doubled Nd-YLF laser (Coherent, Inc., Santa Clara, California, Model Antares) pumping a picosecond DCM [4-dicyanomethylene-2-methyl-6-(*p*-dimethylaminostyryl)-4H-pyran] dye laser (Coherent, Inc., Santa Clara, California, Model 700) was used as the multifrequency excitation source. The same multifrequency phase fluorometer was used to determine the lifetime of Gel/Mount-suspended Crimson spheres. A lifetime of 4.09 ns was obtained, and it compares favorably with our image result of 3.59 ns. Note that, in Fig. 3(a), the harmonic-amplitude image of the cross-correlation signal reveals a ringlike structure in the fluorescence distribution. The edge of the sphere contains a higher concentration of dye than does its interior. This radial dye gradient has been known to exist for the spheres manufactured by our supplier and has been well illustrated by confocal microscopy.[20] Our image of the ring structure thus reveals the axial depth discrimination capability of pump–probe microscopy to be comparable with that of confocal imaging.

Another system that we imaged with our laser-diode-based pump–probe microscopy was TOTO-3–labeled mouse STO cells. TOTO-3 (Molecular Probes, Inc., Eugene, Oregon) is an effective nucleic acid label with absorption and emission maxima at 642 and 660 nm, respectively. The spectral properties of TOTO-3 allow the 635-nm pump laser diode to excite the fluorescent sample and the 680-nm probe laser diode to induce stimulated emission from excited TOTO-3–labeled molecules. The final labeling solution of TOTO-3 is 20 μM, and examples of labeled nuclei are shown in Fig. 4. As in the case for the imaging of the Crimson fluorescent spheres, Nile Blue was used as a fluorescence-lifetime reference compound. Analysis shows that the TOTO-3–labeled nuclei have a lifetime of approximately 1.81 ns.

5. Conclusion

We have successfully demonstrated the use of intensity-modulated laser diodes for applications in frequency-domain pump–probe fluorescence microscopy. By using Nile Blue as a fluorescence-lifetime reference compound, we imaged two fluorescent samples and determined their lifetimes. The 4.0-μm Crimson spheres were shown to have a lifetime of 3.59 ns, and 1.81 ns was the lifetime determined for the TOTO-3–labeled mouse STO nuclei. Pump–probe microscopy that is implemented in this fashion has the characteristic confocal-like sectioning effect, and the capability of measuring the cross-correlation signal at 5 kHz demonstrates that fast photodetectors are not necessary for 80-MHz lifetime measurements. The ability to perform pump–probe imaging with inexpensive laser diodes shows that, with advances in laser-diode technology, inexpensive blue–green laser diodes can soon be utilized in this novel form of microscopy for high-frequency time-resolved microscopic imaging with confocal-like quality.

This study was supported by the National Institutes of Health (RR03155). We would also like to thank Matt Wheeler and the laboratory personnel at the University of Illinois at Urbana-Champaign for their generous support in providing us with the mouse STO cells.

Address correspondence to E. Gratton, Department of Physics, University of Illinois at Urbana-Champaign, 1110 West Green Street, Urbana, Illinois 61801.

References

1. D. K. Evans, ed., *Laser Applications in Physical Chemistry* (Marcel Dekker, New York, 1989).
2. G. R. Fleming, *Chemical Applications of Ultrafast Spectroscopy* (Oxford U. Press, New York, 1986).
3. F. E. Lytle, R. M. Parish, and W. T. Barnes, "An introduction to time-resolved pump–probe spectroscopy," Appl. Spectrosc. **39,** 444–451 (1985).
4. J. Zhou, G. Taft, C. P. Huang, I. P. Christov, H. C. Kapteyn,

and N. M. Murnane, "Sub-10 fs pulse generation in Ti:sapphire: capabilities and ultimate limits," in *Ultrafast Phenomena IX*, P. F. Barbara, W. H. Knox, G. A. Mourou, and A. H. Zewail, eds. (Springer-Verlag, Berlin, 1995), pp. 39–40.
5. L. Xu, C. Spielmann, F. Krausz, and R. Szipocs, "Ultrabroadband ring oscillator for sub-10-fs pulse generation," Opt. Lett. **21,** 1259–1261 (1996).
6. I. P. Christov, V. Stoev, M. M. Murnane, and H. C. Kapteyn, "Sub-10-fs operation of Kerr-lens mode-locked lasers," Opt. Lett. **21,** 1493–1495 (1996).
7. R. M. Hochstrasser and C. K. Johnson, "Biological processes studied by ultrafast laser techniques," in *Ultrashort Laser Pulses*, W. Kaiser, ed. (Springer-Verlag, New York, 1988), pp. 357–417.
8. P. A. Elzinga, R. J. Kneisler, F. E. Lytle, G. B. King, and N. M. Laurendeau, "Pump–probe method for fast analysis of visible spectral signatures utilizing asynchronous optical sampling," Appl. Opt. **26,** 4303–4309 (1987).
9. P. A. Elzinga, F. E. Lytle, Y. Jian, G. B. King, and N. M. Laurendeau, "Pump–probe spectroscopy by asynchronous optical sampling," Appl. Spectrosc. **41,** 2–4 (1987).
10. J. R. Lakowicz, I. Gryczynski, V. Bogdanov, and J. Kusba, "Light quenching and fluorescence depolarization of Rhodamine-B and applications of this phenomenon to biophysics," J. Phys. Chem. **98,** 334–342 (1994).
11. J. Kusba, V. Bogdanov, I. Gryczynski, and J. R. Lakowicz, "Theory of light quenching: effects on fluorescence polarization, intensity, and anisotropy decays," Biophys. J. **67,** 2024–2040 (1994).
12. C. Y. Dong, P. T. C. So, T. French, and E. Gratton, "Fluorescence lifetime imaging by asynchronous pump–probe microscopy," Biophys. J. **69,** 2234–2242 (1995).
13. C. Y. Dong, P. T. C. So, C. Buehler, and E. Gratton, "Spatial resolution in scanning pump–probe fluorescence microscopy," Optik **106,** 7–14 (1997).
14. C. Buehler, C. Y. Dong, P. T. C. So, and E. Gratton, "Time-resolved polarization imaging by pump–probe (stimulated emission) fluorescence microscopy," Biophys. J. **79,** 536–549 (2000).
15. M. Born and E. Wolf, *Principles of Optics*, 5th ed. (Pergamon, Oxford, UK, 1985).
16. C. J. R. Sheppard and M. Gu, "Image formation in two-photon fluorescence microscopy," Optik **86,** 104–106 (1990).
17. M. Gu and C. J. R. Sheppard, "Effects of a finite-sized pinhole on 3D image formation in confocal two-photon fluorescence microscopy," J. Mod. Opt. **40,** 2009–2024 (1993).
18. I. J. Cox, C. J. R. Sheppard, and T. Wilson, "Superresolution by confocal fluorescent microscopy," Optik **60,** 391–396 (1982).
19. J. R. Lakowicz, *Principles of Fluorescence Spectroscopy* (Plenum, New York, 1983).
20. R. P. Haugland, *Handbook of Fluorescent Probes and Research Chemicals*, 5th ed., K. D. Larison, ed. (Molecular Probes, Eugene, Ore., 1989).